Synthesis, Photophysical and Nonlinear Optical Properties of a Series of Ball-type Phthalocyanines in Solution and Thin Films

Njemuwa Nwaji, John Mack, Jonathan Britton, Tebello Nyokong*

Department of Chemistry, Rhodes University, Grahamstown 6140, South Africa

Supplementary Information

Theoretical Calculations

The optimized structures were obtained for one of the possible isomers of **4-6** by using the B3LYP functional of the Gaussian 09 software package with SDD basis sets [1]. The hexadecane side chains were excluded to simplify the calculations. Six different isomers were calculated for **4** to study the effect of changing the points of attachment of the bridging substituents. TD-DFT calculations were carried out using the CAM-B3LYP functional with SDD basis sets. The CAM-B3LYP functional contains a long range connection that provides more accurate results for transitions with significant charge transfer character [2].

Photophysical and nonlinear optical studies.

Fluorescence and triplet quantum yields*:* The fluorescence (Φ_F) and triplet state (Φ_T) quantum yields were determined using the comparative methods as reported in literature [3-5], using ZnPc as a standard (Φ_F = 0.20) [3] and (Φ_T = 0.65 [5] in DMSO.

Nonlinear Optical Measurement: The nonlinear optical behaviour of the synthesized complexes were investigated by using the open aperture Z-scan technique and the data were analyzed in the manner reported by Sheik-Bahae *et al* [6,7] using equation (1):

$$T_{(Z)} = \frac{1}{1 + \beta_{eff} L_{eff} (I_{00}/(1 + (z/z_0)^2))} \qquad (1)$$

where $T_{(Z)}$ is the normalized transmittance of the sample, I_{00} is the intensity of the light on focus, β_{eff} is the two-photon absorption coefficient, Z_0 is the diffraction length of the beam, Z is the sample position with respect to input intensity and L_{eff} is the effective length for two photon absorption in a sample of path length L and is determined using equation (2).

$$l_{eff} = \frac{1 - e^{-\alpha l}}{\alpha} \qquad (2)$$

where α is the linear absorption coefficient. Since equation (1) is not generally suited to directly fit experimental data, a numerical form of equation (1) which is equation (3), was employed to fit the experimental data.

$$T_{(z)} = 0.363e^{\left(\frac{-q(z)}{5.60}\right)} + 0.286e^{\left(\frac{-q(z)}{1.21}\right)} + 0.213e^{\left(\frac{-q(z)}{24.62}\right)} + 0.096e^{\left(\frac{-q(z)}{115.95}\right)} + 0.038e^{\left(\frac{-q(z)}{965.08}\right)} \qquad (3)$$

The excited state cross-section (δ_{exc}) was obtained by fitting the Z-scan experimental data to equation (4):

$$T_{Norm} = \frac{In\left(1 + \left(q/\left(1 + X^2\right)\right)\right)}{q/\left(1 + X^2\right)} \quad (4)$$

where q is a dimensionless parameter that is given by equation 5:

$$q = \frac{\alpha\delta_{exc}}{2hv} F_0 L_{eff} \quad (5)$$

where T_{Norm} is the normalized transmittance, F_0 (J/cm^2) is the total fluence on axis, h is the Planck's constant, v is the frequency of the laser beam, and $\chi = z/z_0$.

Imaginary third-order susceptibility ($I_m[\chi^{(3)}]$) values were calculated using equation (6) [**8,9**]:

$$I_m[\chi]^3 = \frac{n^2 \varepsilon_0 C \lambda \beta_{eff}}{2\pi} \quad (6)$$

where n and c are the linear refractive index, and c is the speed of light, ε_0 is the permittivity of free space and λ is the wavelength of the laser.

The second order hyperpolarizability (γ), which indicates the nonlinear absorption per mole is related to the imaginery third order susceptibility by equation (7).

$$\gamma = \frac{I_m\left[\chi^3\right]}{f^4 C_{mol} N_A} \quad \textbf{(7)}$$

where C_{mol} is the molar concentration of the active species in the triplet state, ƒ (the Lorentz local field enhancement factor) = $n^2 + 2)/3$ (where n is the refractive index of the sample), and N_A is the Avogadro's constant.

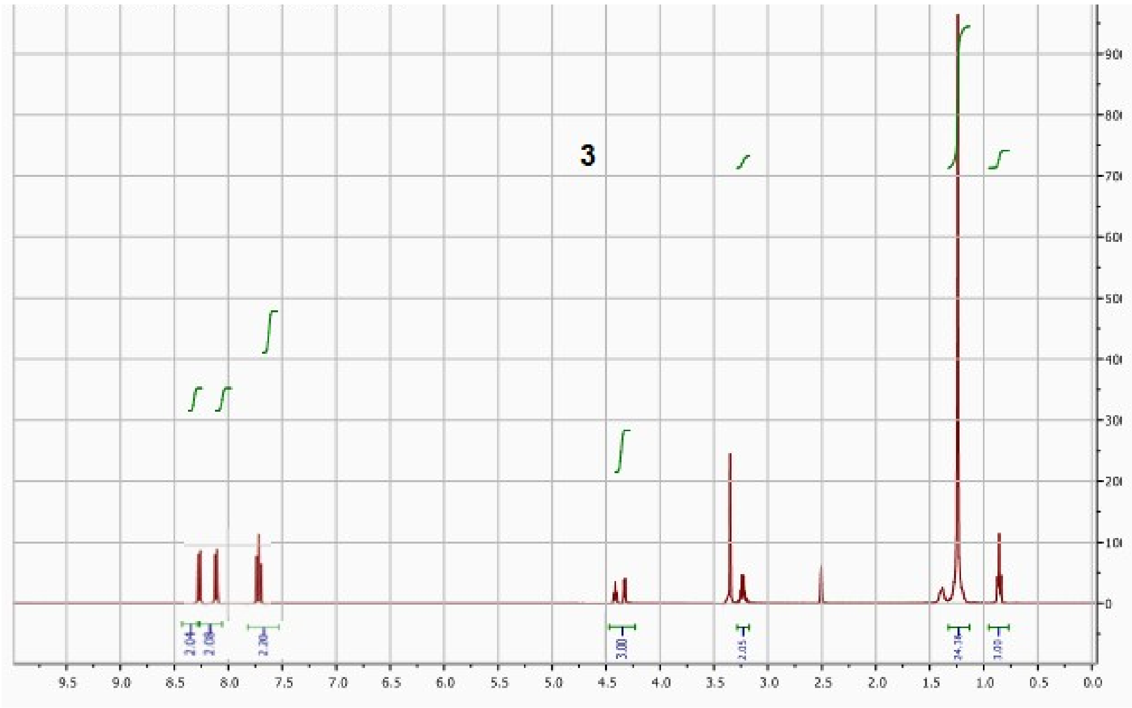
3
90
80
70
60
50
40
30
20
10
0
2.04
2.08
2.30
3.00
2.05
24.16
3.00
9.5
9.0
8.5
8.0
7.5
7.0
6.5
6.0
5.5
5.0
4.5
4.0
3.5
3.0
2.5
2.0
1.5
1.0
0.5
0.0

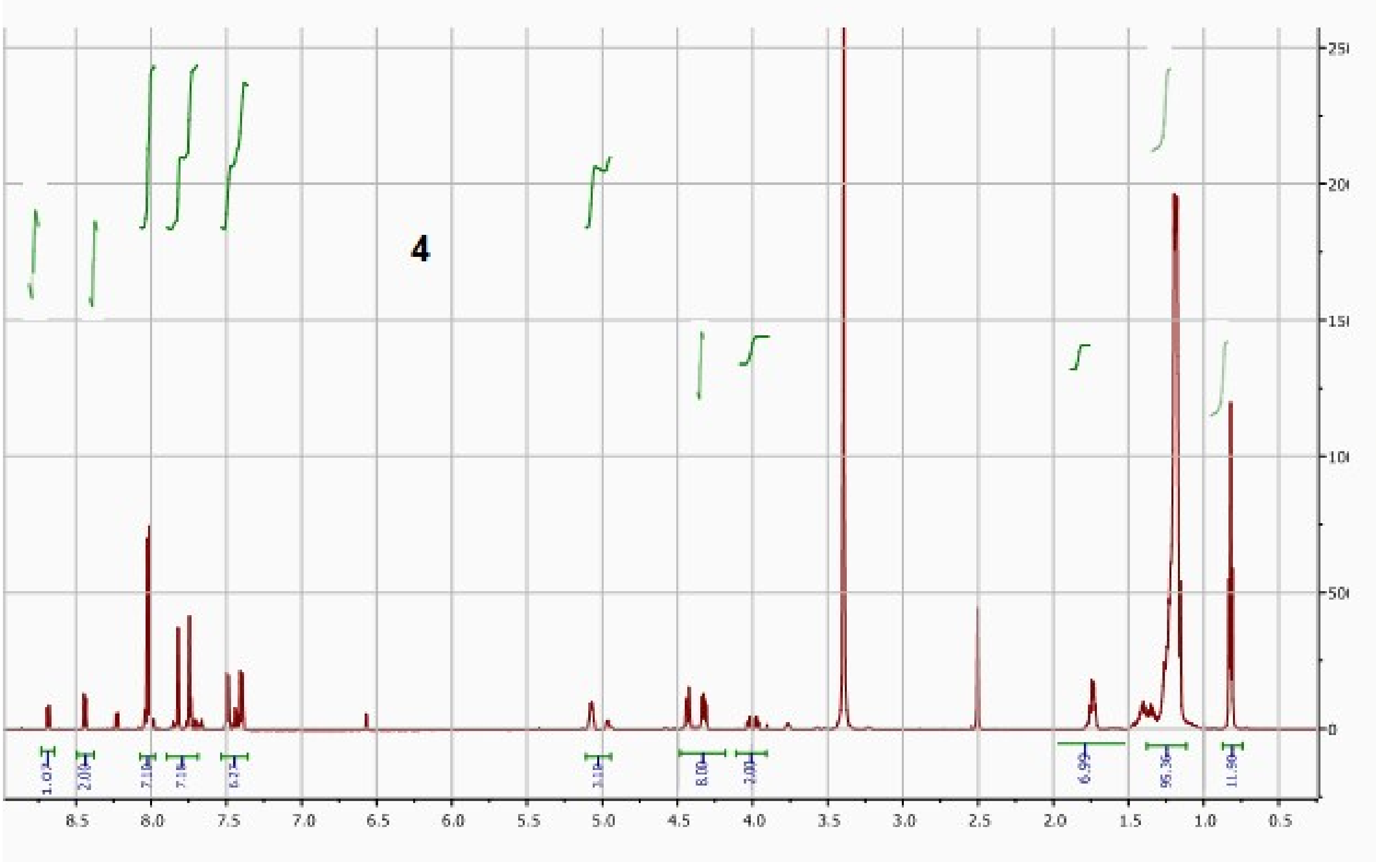
4
25
20
15
10
50
0
1.07
2.00
7.10
7.18
6.27
3.10
8.00
2.00
6.99
95.36
11.60
8.5
8.0
7.5
7.0
6.5
6.0
5.5
5.0
4.5
4.0
3.5
3.0
2.5
2.0
1.5
1.0
0.5

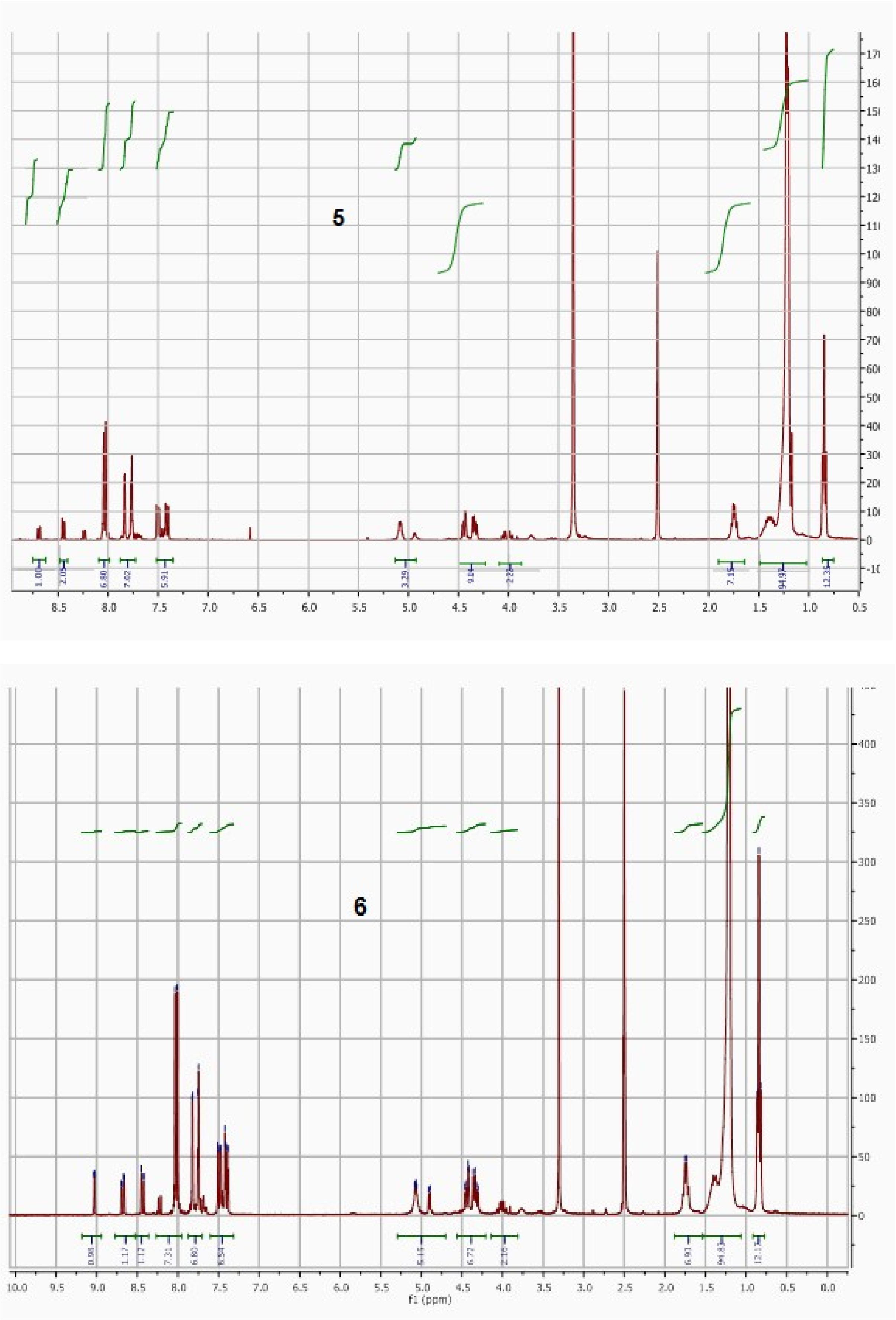

Fig S1: ^{1}H NMR spectrum of complex **3-6** in DMSO

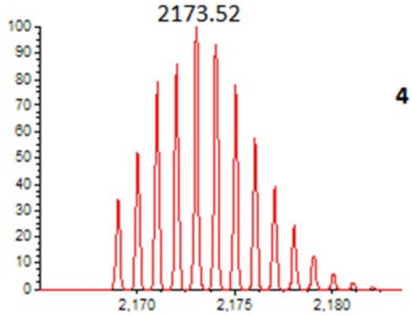

4

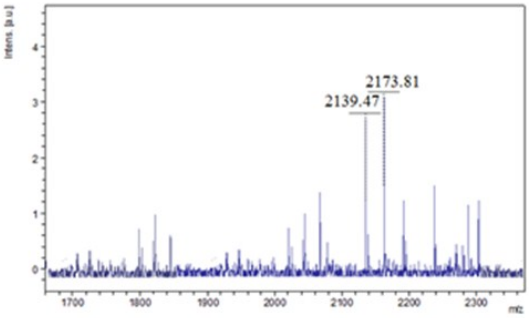

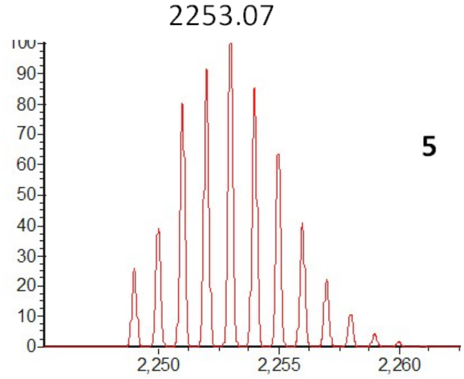

5

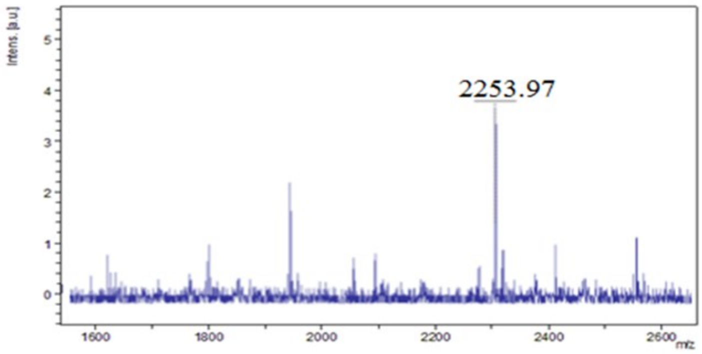

6

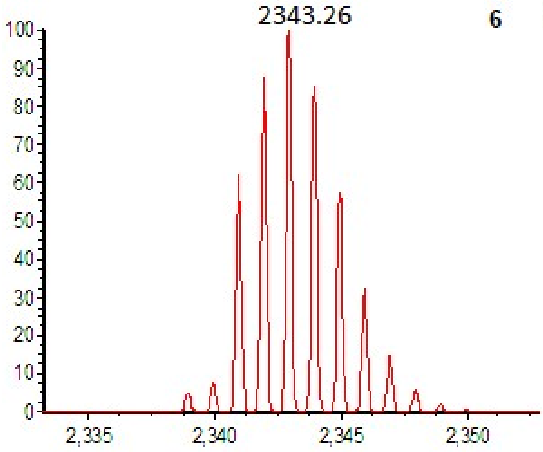

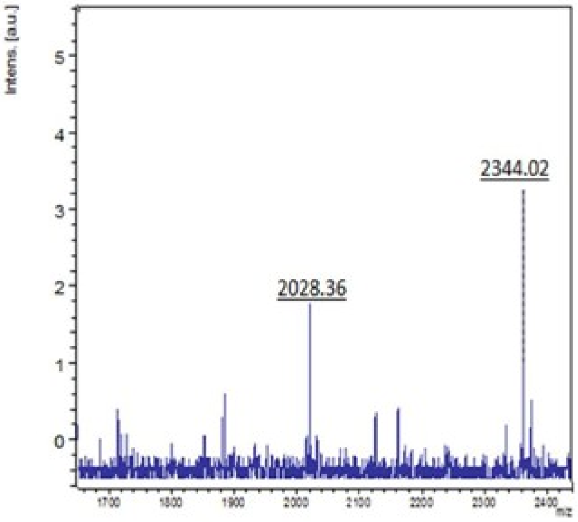

Fig S2: Simulated isotopic distribution (left) and experimental MALDI-TOF mass spectrometry of complex **4-6**

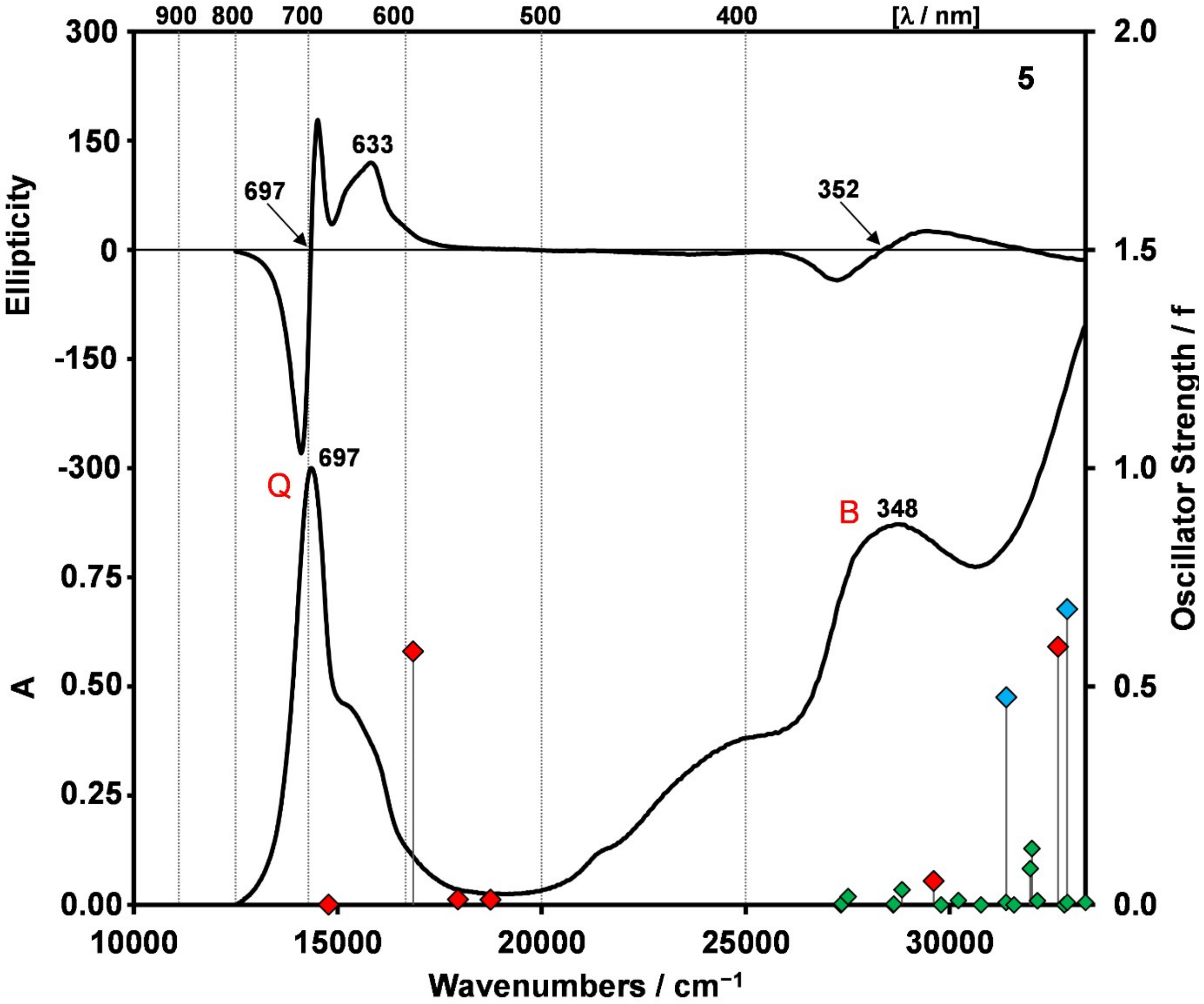

Fig. S3: Absorption spectra and MCD spectra of **5** in THF. The calculated TD-DFT spectrum of the isomer of **5** with four 3,3-position attachments (**Fig. S5**) is plotted against a secondary axis. Red diamonds are used to highlight bands associated with the Q and B bands of Gouterman's 4-orbital model,[10] while blue diamonds are used for transitions associated with what would be the $2a_{2u}$ MO of the Pc rings, if D_{4h} symmetry were assumed.

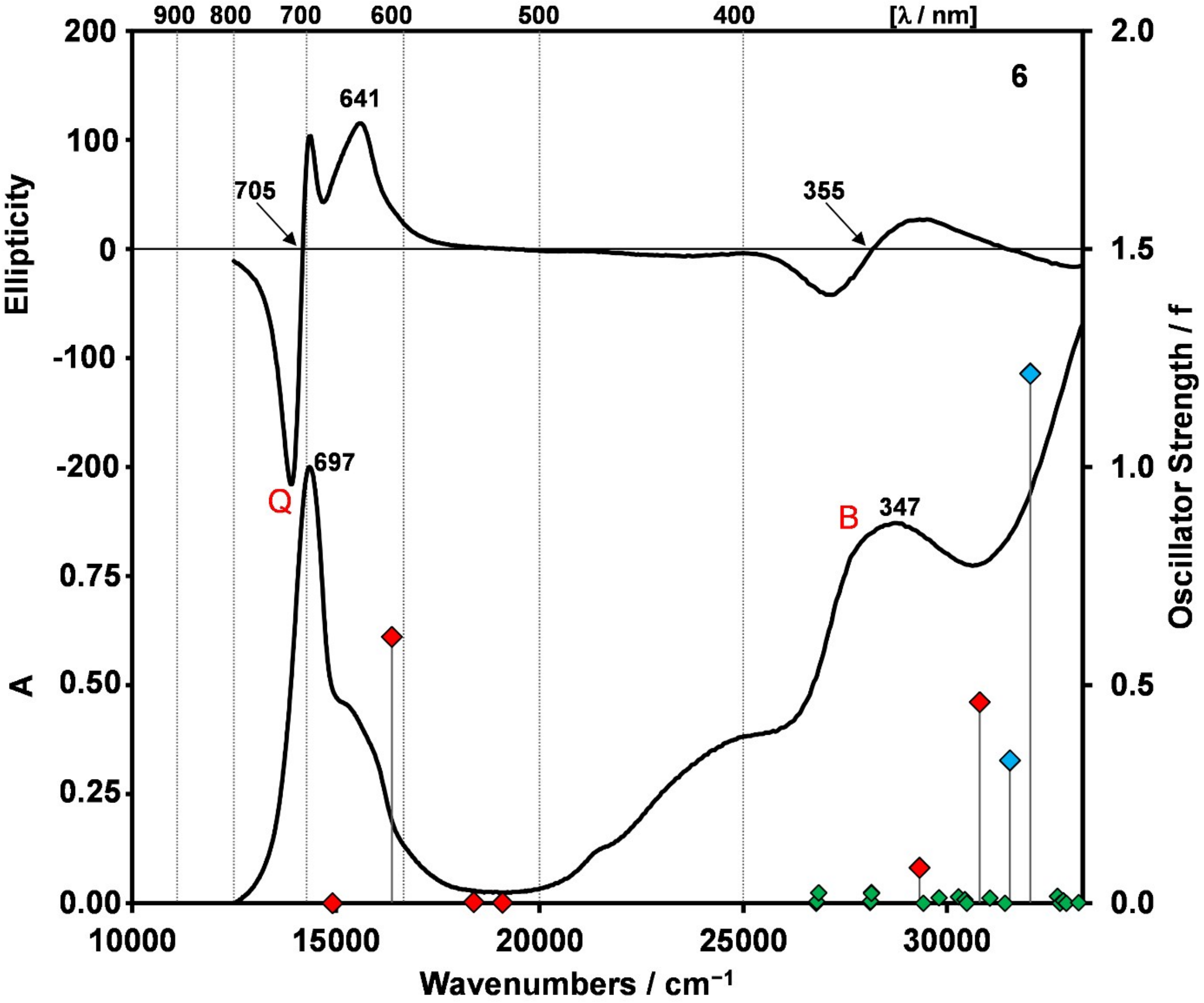

Fig. S4: Absorption spectra and MCD spectra of **6** in THF. The calculated TD-DFT spectrum of the isomer of **6** with four 3, 3-position attachments (**Fig. S5**) is plotted against a secondary axis. Red diamonds are used to highlight bands associated with the Q and B bands of Gouterman's 4-orbital model,[10] while blue diamonds are used for transitions associated with what would be the $2a_{2u}$ MO of the Pc rings, if D_{4h} symmetry were assumed.

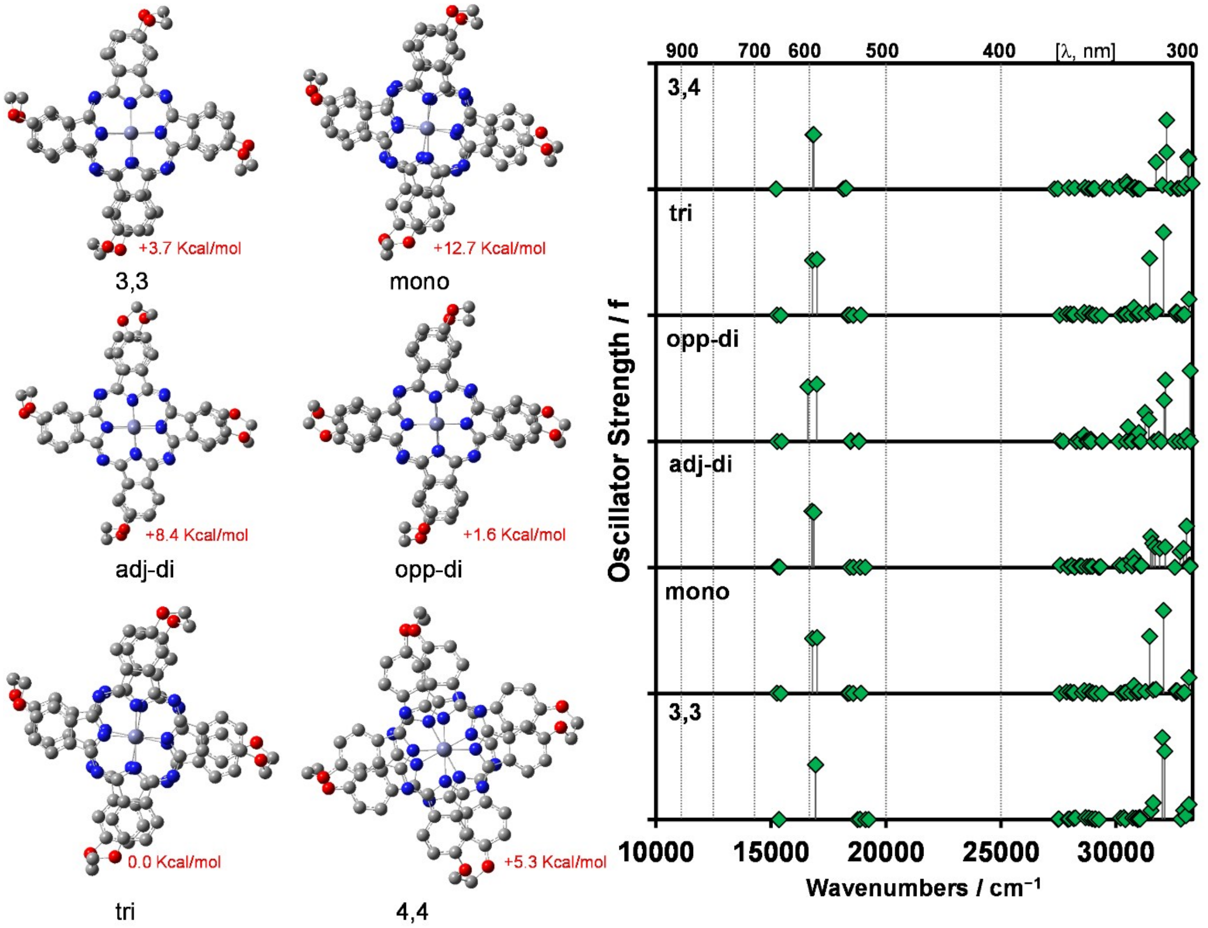

Fig. S5: The structures and predicted relative energies calculated for B3LYP optimized geometries at the CAM-B3LYP/6-31G(d) level of theory for isomers of **4** with only either 3,3- and 3,4- attachments (**3,3** and **3,4**), and structures with both types of attachment arranged in a 3:1 manner (**mono**), in oppositely and adjacently arranged 2:2 structure (**adj-di** and **opp-di**), and a 1:3 manner (**tri**). The hydrogen atoms are omitted for clarity.

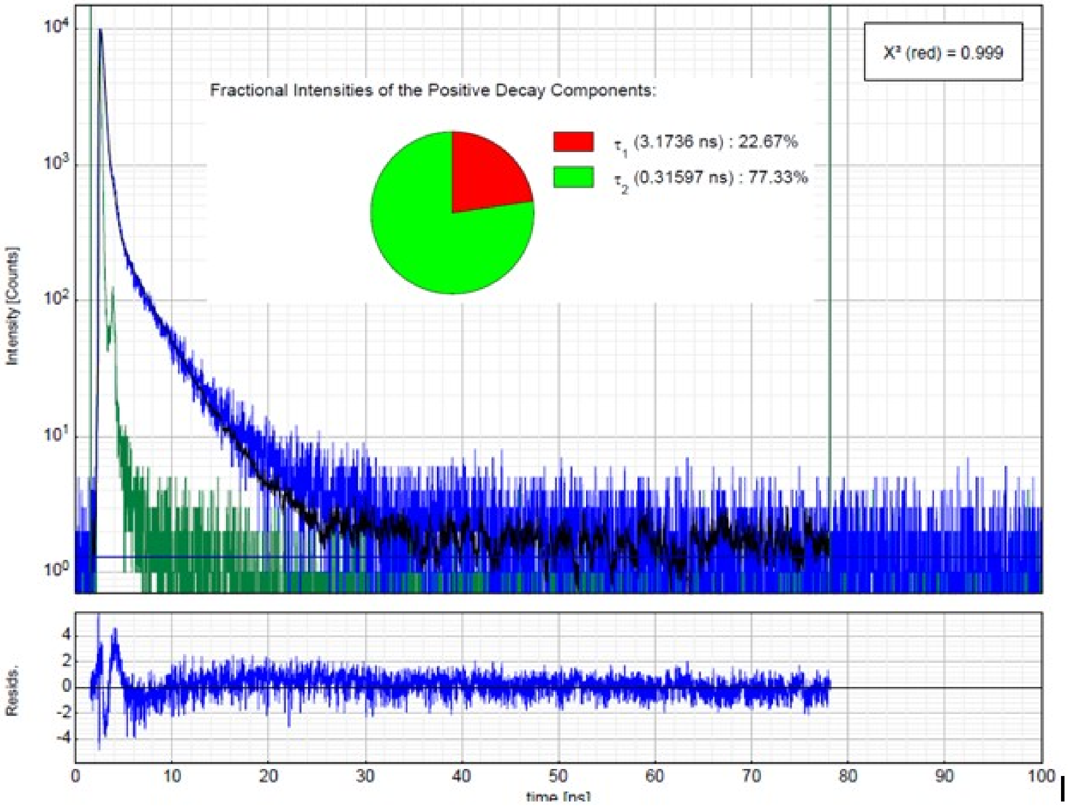

Fig. S6: Time correlated single photon counting (TCSP) lifetime curve for **6** showing two lifetimes.

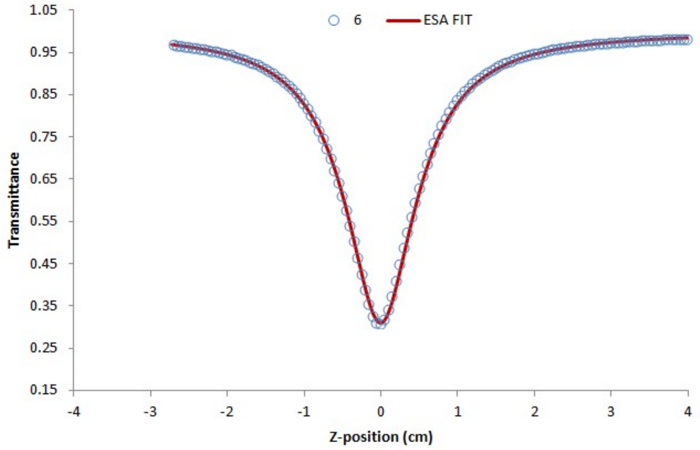

Fig S7: Representative open-aperture Z-scan transmittance of **6** fitted to the ESA absorption state cross-section as a function of sample position.

Table S1. TD-DFT spectra of the B3LYP optimized geometries for the isomers of **4-6** with with four 3,3-position attachments calculated with the CAM-B3LYP functional and SDD basis sets.

4

Band[a]	#[b]	Calc[c]			Exp[d]		Wave Function[e] =
----	**1**	----	----	----	----	----	Ground State
Q	**4**	16.9	590	(0.65)	14.7	681	**89% $1a_{1u} \rightarrow 1e_g^*$**; …
	5	16.9	590	(0.65)	14.7	681	**90% $1a_{1u} \rightarrow 1e_g^*$**; …
B	**33**	32.0	312	(0.97)	28.7	348	**30% $1a_{2u} \rightarrow 1e_g^*$**; 26% $1b_{2u} \rightarrow 1e_g^*$; …
	34	32.1	311	(0.81)	28.7	348	**42% $1a_{2u} \rightarrow 1e_g^*$**; …

5

Band[a]	#[b]	Calc[c]			Exp[d]		Wave Function[e] =
----	**1**	----	----	----	----	----	Ground State
Q	**4**	16.8	594	(0.58)	14.3	697	**90% $1a_{1u} \rightarrow 1e_g^*$**; …
	5	16.8	594	(0.58)	14.3	697	**90% $1a_{1u} \rightarrow 1e_g^*$**; …
--	**18**	29.6	338	(0.05)	---	---	**68% $1a_{2u} \rightarrow 1e_g^*$**; 13% $1b_{2u} \rightarrow 1e_g^*$; …
	19	29.6	338	(0.05)	---	---	**68% $1a_{2u} \rightarrow 1e_g^*$**; 13% $1b_{2u} \rightarrow 1e_g^*$; …
--	**24**	31.4	319	(0.48)	---	---	**38% $1a_{2u} \rightarrow 1e_g^*$**; 31% $2a_{2u} \rightarrow 1e_g^*$; …
	25	31.4	319	(0.48)	---	---	**38% $1a_{2u} \rightarrow 1e_g^*$**; 31% $2a_{2u} \rightarrow 1e_g^*$; …
B	**33**	32.7	306	(0.59)	28.2	355	**31% $1a_{2u} \rightarrow 1e_g^*$**; 27% $1b_{1u} \rightarrow 1e_g^*$; 16% $2a_{2u} \rightarrow 1e_g^*$; …
	34	32.7	306	(0.59)	28.2	355	**31% $1a_{2u} \rightarrow 1e_g^*$**; 27% $1b_{1u} \rightarrow 1e_g^*$; 16% $2a_{2u} \rightarrow 1e_g^*$; …
--	**36**	32.9	304	(0.68)	---	---	37% $2a_{2u} \rightarrow 1e_g^*$; 28% $1b_{1u} \rightarrow 1e_g^*$; **19% $1a_{2u} \rightarrow 1e_g^*$**; …
	37	32.9	304	(0.68)	---	---	37% $2a_{2u} \rightarrow 1e_g^*$; 28% $1b_{1u} \rightarrow 1e_g^*$; **19% $1a_{2u} \rightarrow 1e_g^*$**; …

6

Band[a]	#[b]	Calc[c]			Exp[d]		Wave Function[e] =
----	**1**	----	----	----	----	----	Ground State
Q	**4**	16.4	611	(0.61)	14.2	705	**88% $1a_{1u} \rightarrow 1e_g^*$**; …
	5	16.4	611	(0.61)	14.2	705	**88% $1a_{1u} \rightarrow 1e_g^*$**; …
--	**18**	29.3	341	(0.08)	---	---	**67% $1a_{2u} \rightarrow 1e_g^*$**; …
	19	29.3	341	(0.08)	---	---	**67% $1a_{2u} \rightarrow 1e_g^*$**; …
--	**27**	30.8	325	(0.46)	---	---	**34% $1a_{2u} \rightarrow 1e_g^*$**; 31% $2a_{2u} \rightarrow 1e_g^*$; …
	28	30.8	325	(0.46)	---	---	**34% $1a_{2u} \rightarrow 1e_g^*$**; 31% $2a_{2u} \rightarrow 1e_g^*$; …
--	**31**	31.5	317	(0.33)	---	---	56% $2a_{2u} \rightarrow 1e_g^*$; …
	32	31.5	317	(0.33)	---	---	56% $2a_{2u} \rightarrow 1e_g^*$; **12% $1a_{2u} \rightarrow 1e_g^*$;** …
B	**33**	32.0	312	(1.21)	28.4	352	45% $2a_{2u} \rightarrow 1e_g^*$; **15% $1a_{2u} \rightarrow 1e_g^*$**; …
	34	32.0	312	(1.21)	28.4	352	45% $2a_{2u} \rightarrow 1e_g^*$; **15% $1a_{2u} \rightarrow 1e_g^*$**; …

a – Band assignment described in the text. b – The number of the state assigned in terms of ascending energy within the TD-DFT calculation. c – Calculated band energies (10^3.cm^{-1}), wavelengths (nm) and oscillator strengths in parentheses (f). d – Observed energies (10^3.cm^{-1}) and wavelengths (nm) in **Figures 2, S3** and **S4**. e – The wave functions based on the eigenvectors predicted by TD-DFT. One-electron transitions associated with MOs associated with the four frontier π-MOs of Gouterman's 4-orbital model[S1] are highlighted in bold. The symmetry notations used refer to the D_{4h} symmetry of the parent monomeric complexes.

References

1. M. J. Frisch, G. W. Trucks, H. B. Schlegel, G. E. Scuseria, M. A. Robb, J. R. Cheeseman, G. Scalmani, V. Barone, B. Mennucci, G. A. Petersson, H. Nakatsuji, M. Caricato, X. Li, H. P. Hratchian, A. F. Izmaylov, J. Bloino, G. Zheng, J. L. Sonnenberg, M. Hada, M. Ehara, K. Toyota, R. Fukuda, J. Hasegawa, M. Ishida, T. Nakajima, Y. Honda, O. Kitao, H. Nakai, T. Vreven, J. A. Montgomery, Jr., J. E. Peralta, F. Ogliaro, M. Bearpark, J. J. Heyd, E. Brothers, K. N. Kudin, V. N. Staroverov, R. Kobayashi, J. Normand, K. Raghavachari, A. Rendell, J. C. Burant, S. S. Iyengar, J. Tomasi, M. Cossi, N. Rega, J. M. Millam, M. Klene, J. E. Knox, J. B. Cross, V. Bakken, C. Adamo, J. Jaramillo, R. Gomperts, R. E. Stratmann, O. Yazyev, A. J. Austin, R. Cammi, C. Pomelli, J. W. Ochterski, R. L. Martin, K. Morokuma, V. G. Zakrzewski, G. A. Voth, P. Salvador, J. J. Dannenberg, S. Dapprich, A. D. Daniels, Ö. Farkas, J. B. Foresman, J. V. Ortiz, J. Cioslowski, and D. J. Fox, Gaussian 09, Revision E.01 Gaussian, Inc., Wallingford CT, 2009
2. R. J. Magyar, S. J. Tretiak, *J. Chem. Theory Comput.* 2007, **3**, 976–987
3. A. Ogunsipe, J. Chen, T. Nyokong, *New J. Chem*. 2004, **28,** 822–827.
4. S. Fery-Forgues, D. Lavabre, *J. Chem. Educ*. 1999, **76**, 1260-1263.
5. T.H. Tran-Thi, C. Desforge, C. Thiec, *J. Phys. Chem.* 1989, **93**, 1226-1233.
6. M. Sheik-Bahae, A.A. Said, T.H. Wei, D.J. Hagan, E.W. Van Stryland, *IEEE J. Quantum Electron*. 1990, **26**, 760–769.
7. M. Sheik-bahae, *Opt. Lett*. 1989, **4**, 955–957.
8. E.M. García, S.M. O'Flaherty, E.M. Maya, G. de la Torre, W. Blau, P. Vázqueza, *J. Mater. Chem*. 2003, **13**, 749–753.
9. E.W. Van Stryland, M. Sheik-Bahae, Z-Scan Measurements of Optical Nonlinearities, *Charact. Tech. Tabul. Org. Nonlinear Mater.* (1998) 655–692.
10. Gouterman M. Optical Spectra and Electronic Structure of Porphyrins and Related Rings. In *The Porphyrins*, vol. III, Dolphin D. (Ed.) Academic Press: New York, 1978, 1-165.